

CHEMISTRY

A European Journal

A Journal of



Accepted Article

Title: Supramolecular Hydrogels Based on Minimalist Amphiphilic Squaramide-Squaramates for Controlled Release of Zwitterionic Biomolecules

Authors: Antonio Costa, Carlos López, Marta Ximenis, Francisca Orvay, and Carmen Rotger

This manuscript has been accepted after peer review and appears as an Accepted Article online prior to editing, proofing, and formal publication of the final Version of Record (VoR). This work is currently citable by using the Digital Object Identifier (DOI) given below. The VoR will be published online in Early View as soon as possible and may be different to this Accepted Article as a result of editing. Readers should obtain the VoR from the journal website shown below when it is published to ensure accuracy of information. The authors are responsible for the content of this Accepted Article.

To be cited as: *Chem. Eur. J.* 10.1002/chem.201701029

Link to VoR: <http://dx.doi.org/10.1002/chem.201701029>

Supported by
ACES

WILEY-VCH

Supramolecular Hydrogels Based on Minimalist Amphiphilic Squaramide-Squaramates for Controlled Release of Zwitterionic Biomolecules

Carlos López, Marta Ximenis, Francisca Orvay, Carmen Rotger and Antonio Costa*

Abstract: Supramolecular hydrogels with tunable properties have innovative applications in biomedicine, catalysis and materials chemistry. Herein, we have designed minimalist low molecular weight hydrogelators based on squaramide and squaramic acid motifs. Our approach benefits from the high acidity of squaramic acids and the aromaticity of squaramides. Moreover, the substituents on the aryl ring tune the π density of the aryl-squaramide motif. Thus, we successfully prepared materials featuring distinct thermal and mechanical properties. The hydrogel ($G' \approx 400$ Pa, $G'' \approx 57$ Pa; at 1.0 % w/v; 1 Hz) obtained from the 4-nitrophenylsquaramide motif **1** is thermoreversible ($T = 57$ °C at 0.2 % w/v), thixotropic, self-healable and undergoes irreversible shrinking in response to saline stress. Furthermore, the hydrogel is injectable and can be loaded with substantial amounts (5:1 excess molar ratio) of zwitterionic biomolecules such as L-carnitine, GABA or DL-Ala-DL-Ala, without any loss of structural integrity. Then, the release of these molecules can be modulated by saline solutions.

Supramolecular hydrogels,^[1] formed through the non-covalent assembly of low molecular weight hydrogelators (LMWHs), are materials of scientific interest for innovative applications in biomedicine,^[2] catalysis,^[3] and material chemistry.^[4] Because of their essential reversible character, water gelation by small molecules provides gel-to-sol transitions and a rapid response to external stimuli. Of equal importance, appropriate design and the limited synthetic effort required in their preparation allow effective control over the assembled structures and their responses on the macroscopic level. This control is highly desirable for practical applications as it enables the creation of hydrogels with tunable mechanical properties.^[1a]

Because of the complexity of the self-assembly phenomenon, the *ex novo* design of supramolecular hydrogels using LMWHs is challenging. There is a consensus that LMWHs possess amphiphilicity and require non-covalent interactions such as π - π , hydrogen bonding, and charge interactions among the constituent molecules to build three-dimensional networks in water.^[5] Specifically, peptides and other amide-like compounds,

which contain hydrophilic (charged) and hydrophobic side chains have been successfully used as LMWHs.^[1,6] In this vein, disubstituted squaramides and squaramic acids are advantageous as they can establish synergic hydrogen bonding-aromaticity relationships that control the outcome of the aggregation process^[7] in the solid state^[8] and in solution.^[9] However, N-aryl-substituted squaramic acids^[10] are highly acidic compounds (pKa 0.8-2) that have never used for hydrogel construction. High acidity is crucial when using squaramic acids as the hydrophilic portion of an LMWH because the acidity ensures complete ionization over a broad pH range.^[10a] As with the squaramides, squaramic acid salts (named as squaramates) are moderately aromatic.^[8b] Both, aryl squaramides and aryl squaramates are planar and can form antiparallel stacked dimers in the solid state (Figure 1a, 1b).^[8b,11,12] Overall, the hydrolytic stability^[13] and the aggregation capabilities of squaramides and squaramates, renders their use as synthons for LMWH attractive.

Inspired by the solid-state structures of reported squaramide derivatives, we hypothesized that the combination of aryl-squaramide and aryl-squaramate motifs would enhance the stacking interactions of the resulting squaramide-squaramate ensemble (Figure 1c). Herein, we report that LMWHs based on the squaramide-squaramate couple (Figure 1) self-assemble to form supramolecular hydrogels. The role of the substituents -NO₂ and -CF₃ on the aryl squaramide moiety is intended to modulate the molecular aggregation of the LMWHs to tune the macroscopic properties of the resulting hydrogels.

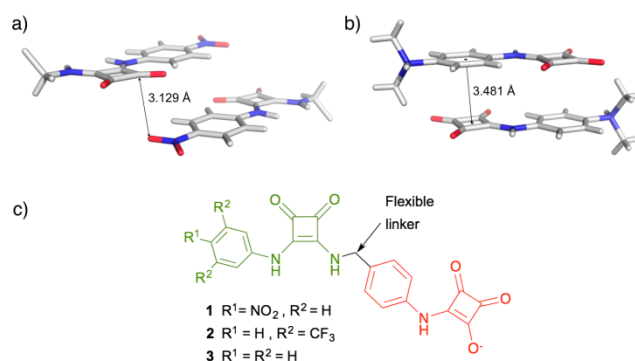


Figure 1. (a) Partial X-ray structure illustrating the planar stacked-offset arrangement of the p-nitrophenyl squaramide motif.^[12] (b) X-ray structure of a phenyl squaramic acid.^[8d] (c) Chemical structures of amphiphilic squaramide-squaramic LMWHs **1-3**.

[a] Carlos López, Marta Ximenis, Francisca, Orvay, Prof. C. Rotger, Prof. A. Costa
 Departament de Química, Facultat de Ciències
 Universitat de les Illes Balears
 Ctra. Valldemossa, Km. 7.5, Palma 07122, Spain
 E-mail: antoni.costa@uib.es

Full synthetic and experimental procedures are provided in the Supporting information which can, as well as the ORCID identification of the author(s) of this article, be found under <http://>

In this work, we synthesized the amphiphilic LMWHs **1-3**. Precursors **1-3** share a common squaramide-squaramate framework but surprisingly show strikingly distinct aggregation properties in water. The addition of NaOH triggers the self-assembly and hydrogelation of **1** ($R_1 = \text{NO}_2$; $R_2 = \text{H}$) in minutes at a pH range from 3-9, with or without heating. The resulting hydrogel **1A** passes the vial inversion test at a relatively low concentration (0.1-0.2 % w/v) (Figure 2a).

Similarly, squaramide **2** ($R_1 = \text{H}$; $R_2 = \text{CF}_3$) also gelifies but requires heating to obtain the hydrogel, and the critical gelation concentration is higher (1.6 % w/v) (Figure 2b and Table S1). However, after similar treatment, squaramide **3** remains as a suspension even with extensive sonication and heating. A comparison of the atomic force microscopy (AFM) images of freshly prepared samples of the hydrogels **1A** and **2A** (Figure 2e, f) reveals marked morphologic differences. Aside from the micrometer-size disordered fibers observed in the two hydrogels, **1A** shows bundled fibrous assemblies composed of one or more strands with an apparent width of 42 nm (2 nm height) (Figure S1). Meanwhile, the morphology of **2A** comprises both right and left-handed helical ribbons with an average diameter of 52 nm twisting around the central axis of the fiber (Figures 2g-j and S2). SEM and TEM images of dried samples of hydrogels **1A** and **2A** confirm the formation of networks of bundled fibers characteristic of hydrogels (Figures 2c,d, S3 and S4). Undoubtedly, the different morphologies of hydrogels **1A** and **2A** and the failure of hydrogel formation of precursor **3** reflect the influence of the peripheral substituents on the self-assembly of the precursor hydrogelators.

To shed light on the initial self-assembly events, we studied the evolution of the ^1H NMR spectra of solutions of **1** (1.0×10^{-3} M) in different $[\text{D}_6]\text{-DMSO}/\text{H}_2\text{O}$ solvent mixtures. Upon increasing the amount of water in the solvent mixture, all aromatic protons exhibit significant upfield shifts (-0.1 to -0.5 ppm), indicating the growing influence of the aromatic stacking interactions that occur in water (Fig. 3). Previously, we have reported that a dynamic equilibrium driven by hydrogen bonding between the monomeric and dimeric forms of **1** exists in $[\text{D}_6]\text{-DMSO}$.^[14] In agreement, the NH proton of the squaramate first moves downfield and then reverses direction, indicating hydrogen bond breaking, in $\text{DMSO}/\text{H}_2\text{O}$ mixtures containing > 50 % of H_2O .

The electrospray high-resolution mass spectrometry ESI(-)HRMS analysis of very diluted solutions of **1-3** ($c \approx 10^{-6}$ M) also provides clues about the aggregation of these precursors. Squaramide **1** shows an intense base peak at m/z 433.0789 assigned to the monomer $[\text{M-H}]^-$ anion with 44 % contribution of the doubly charged dimer, $[\text{2M-2H}]^{2-}$. The base peak of **2** appears at 524.0681 and the contribution of the dimer increases to 68 %. In both cases, several minor peaks at higher m/z assigned to low oligomers were also observed, albeit at a proportion < 5 % compared to the dimer. In contrast, the molecular peak of **3** at m/z 389.3670 contains less than 3 % of dimer thus indicating the low aggregation ability of **3** (Figures S5-S7).

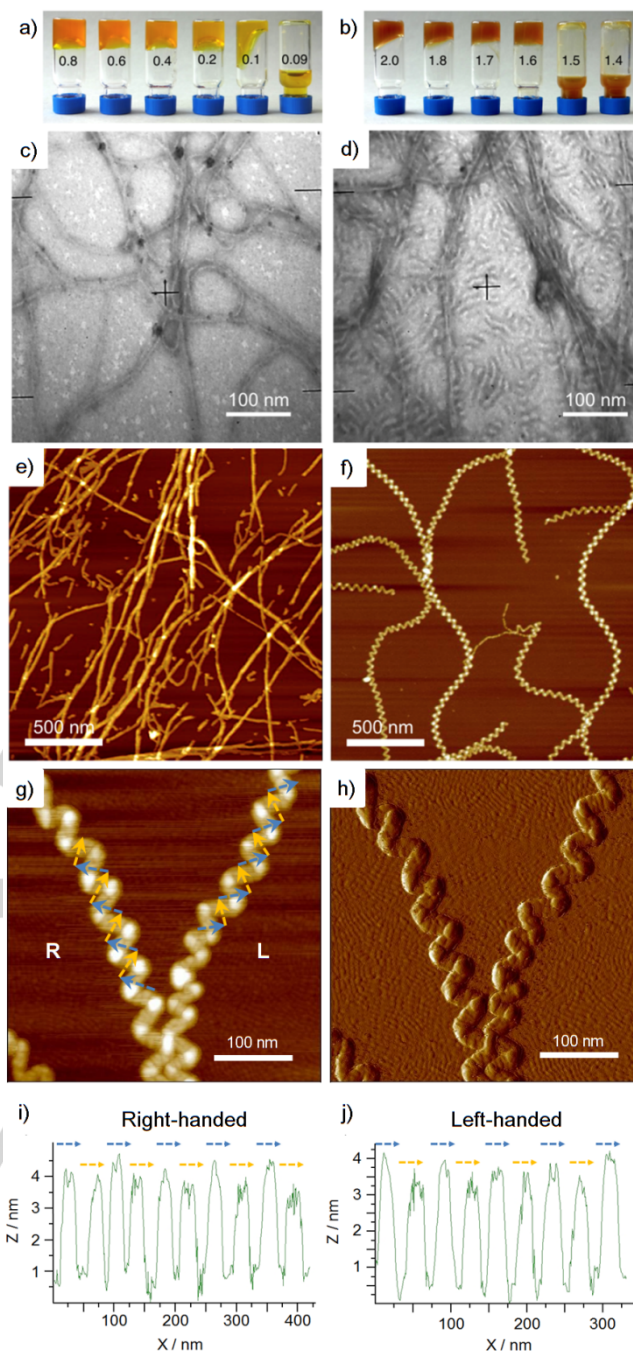


Figure 2. (a, b) Vial inversion tests performed on slow-cooled samples of **1A** and **2A**, after gentle heating at 70°C for 1 h. The values on the vials indicate the % w/v of the hydrogelators **1** and **2**, respectively. (b, c) TEM images of fibrils from self-assembly of **1A** (0.03 % w/v; $c = 0.58$ mM) and **2A** (0.018 % w/v; $c = 0.41$ mM) in water. The hydrogels were negatively stained with 1% w/v phosphotungstic acid before observation. (e, f) AFM images obtained on mica by depositing 60 μL aliquots of diluted hydrogels **1A** (0.015 % w/v; $c = 0.34$ mM) and **2A** (0.015 % w/v; $c = 0.29$ mM), respectively. (g) Enlarged image of two helices, one right-handed (R) and another left-handed (L), and its corresponding amplitude image (h). (i, j) Cross-section profiles plotted following the dash lines of the image (g) indicates the direction of rotation of the two helices. The colors of the dash arrows on each peak are referenced to the correspondent fragment of the cross section.

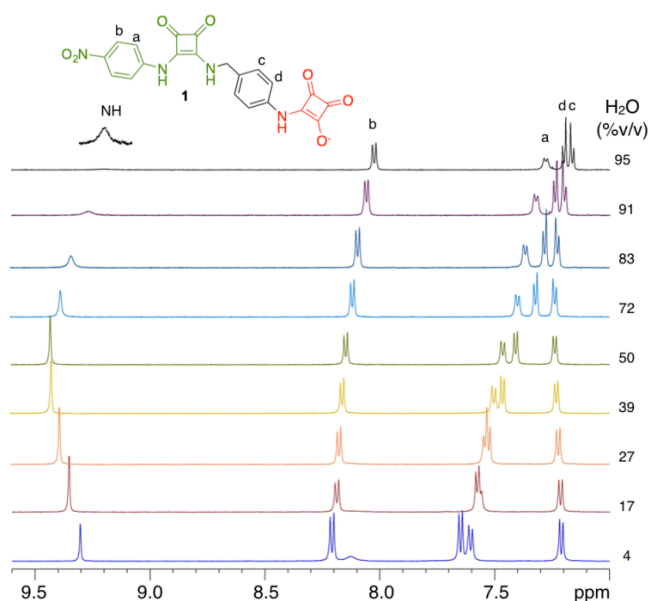


Figure 3. Partial ^1H NMR spectra (300 MHz) of a solution of the sodium salt of **1** (1.0×10^{-3} M) at room temperature in [D6]-DMSO- H_2O solvent mixtures containing increasing percentages of H_2O . All the spectra were registered using WATERGATE pulse sequences for water-suppression.

The formation of aggregates from **1** and **2** was assessed by static light scattering (SLS) and UV-vis measurements. A plot of scattered intensity as a function of concentration displays almost superimposable curves for the two hydrogels (Figure 4a). From these data, the critical aggregation concentration (CAC) at the junction is $8.0 \pm 1.0 \times 10^{-5}$ M similar to that found by UV-vis for **1** (Figure 4b). However, the change between the two lines is not as abrupt as one would expect for a cooperative aggregation model.

To gather further information, we explored the aggregation of hydrogelator **1A** by UV-vis. Hydrogelator **1**, being more soluble than **2**, allows aggregation equilibria to be studied over a broader range of concentrations.

The UV-vis spectra of solutions of **1** in water, registered below the CAC, do not show isosbestic points indicating the absence of other equilibria, i.e., acid-base.^[12a,15] The high-intensity band at 318 nm is common to all squaramide and squaramic derivatives, and hence,^[10] its diagnostic value is minimal. The lowest-energy band appears at approximately 388 nm (Figure 4c), and we assigned it to the $S_0 - S_1$ electronic transition of the 4-nitrophenyl squaramide chromophore. Upon increasing the concentration of **1**, the band at 388 nm vanishes completely, and a new band appears blue-shifted as a shoulder at 355 nm, suggesting H-aggregation. Remarkably, the band at 388 nm reappears upon heating (Figure S9), thus indicating the reversible character of the aggregation and providing clear evidence that the aggregation of **1** involves electronic interactions between the 4-nitrophenyl squaramide chromophores. In agreement, the apparent molar absorption coefficient at 388 nm could be fitted to the isodesmic (equal-K) model of aggregation (Figure 4d), producing an association constant of $800 \pm 75 \text{ M}^{-1}$ which compares well with published values.^[16]

The phenyl substituents of **1** (- NO_2) and **2** (- CF_3), not only modify the initial hydrogel core formation capabilities but strongly

influence their responsiveness to external stimuli such as heat and shear. We analyzed the thermal behavior of hydrogels **1A** and **2A** by differential scanning calorimetry (DSC) and the vial inversion method (Table S2). A DSC thermogram of **1A** (0.25 % w/v) from 25-90°C (Figure S10), exhibits an endothermic peak at $T = 57$ °C. The peak is concentration-dependent and its broad shape reveals the continuous character of the transitions that occur in the hydrogel. Moreover, the hydrogel is thermoreversible, that is, it evolves into solution upon heating and then returns to the hydrogel form upon cooling at room temperature. In contrast, the DSC thermogram of **2A** registered over the same temperature range displays a flat line, indicating that hydrogel **2A** is thermally stable.

We confirmed the hydrogel nature of **1A** and **2A** by conducting dynamic rheological experiments. The frequency-sweep experiments show a value of the storage modulus (G') 10-fold greater than that of the loss modulus (G'') over the entire frequency range (1 % strain; frequency range 0.1-100 Hz), characteristic of viscoelastic fibrous networks (Figure S13). At the same concentration (2 % w/v), the magnitude of the G' modulus for **2A** is ten times greater than that for **1A**, thus demonstrating its greater resistance against mechanical disturbance.

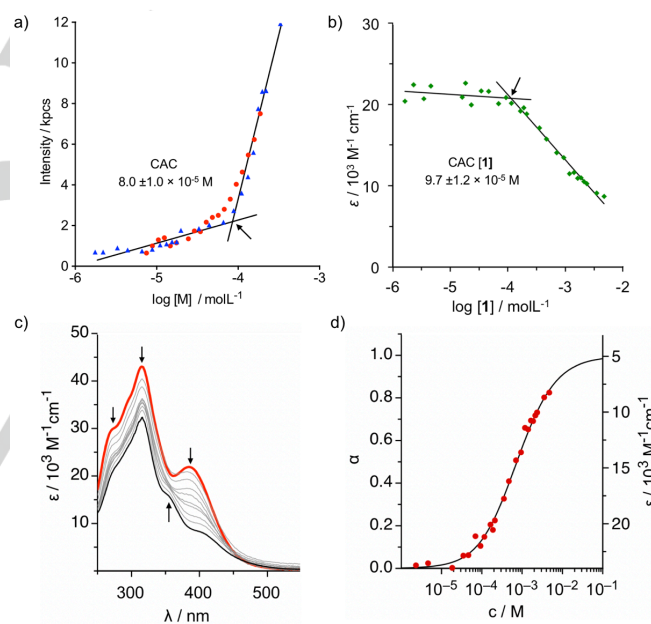


Figure 4. (a) Scattered intensity (s^{-1}) as a function of concentration, $\log[M]$, of **1** (red) and **2** (blue). (b) Molar extinction coefficient of **1** at 390 nm as a function of concentration of **1**. In both cases, the calculated CAC at the line junctions are indicated on the plots. (c) Concentration-dependent UV-vis spectra of hydrogel **1A** obtained in a concentration range between 4.6×10^{-5} (red line) and 7.0×10^{-3} M (black line). The arrows indicate the direction of the movement upon increasing the concentration of **1A**. (d) Molar fraction (α) of aggregated molecules as a function of concentration of the hydrogel **1A**. The line was obtained by fitting the experimental UV-vis data with the isodesmic model.

In order to evaluate the biocompatibility of **1**, U87 cells were subconfluently grown in the presence of hydrogelator **1** at increasing concentrations. The toxicity was evaluated by a luminiscent test. No toxicity was found for concentrations of **1** up to 500 μM (Figure S11). Thus, the lack of toxicity and the weak

stacking interactions that govern the structure of **1A** translate into a set of properties of high interest for biotechnological applications. In addition to being thermoreversible at a relatively low temperature, hydrogel **1A** is thixotropic (its viscosity diminishes under compression); therefore **1A** flows into small channels, and it is readily injectable (Figure 5b and TOC). We assessed the thixotropic behavior of **1A** by applying stepwise cycles of high and low stress to a sample of **1A** (2 % w/v) (Figure 5a). Under low strain, the hydrogel displays a storage modulus an order of magnitude higher than the loss modulus, which is consistent with its gel state. At high strain, both storage and loss moduli drop reaching similar values, indicating a phase transition from gel to a solution.^[17] The application of low strain allowed the moduli to recover rapidly the same magnitudes as before the stress.

When dipped in water, the hydrogel remains unaltered for weeks. However, the addition of saline solutions (such as NaCl, Et₄NCl, KCl, MgCl₂, Me₄NOAc, or acetylcholine chloride) to **1A** causes homogeneous and irreversible shrinking, in such a way that the shrunken gel keeps the shape of its container. The magnitude of the macroscopic phase transition depends on the total concentration of the salt added and its molar ratio to the hydrogelator (Figures 5c and S12). The kinetics of the process is fast since, after four hours from the addition of the salt solution, the hydrogel has shrunk practically to its final volume. When completely shrunken, the stiffness of the resulting hydrogel **1B** increases considerably compared to **1A** (1Hz, $G'_{1B}/G'_{1A} \approx 25$, $G''_{1B}/G''_{1A} \approx 20$) (Figure S14).

Finally, in contrast with the shrinking effect of added salts, hydrogel **1A** can be loaded, with a variety of zwitterionic molecules, such as L-carnitine, GABA and DL-Ala-DL-Ala, without disturbing the hydrogel structure. These molecules can be added in a 5:1 excess molar ratio to **1**, before heating, without disturbing the mechanical stability of the resulting loaded hydrogel. However, the addition of related organic salts, such as tetramethylammonium acetate or acetylcholine chloride to the solution of **1**, causes shrinking of the hydrogel.

The loaded hydrogel can release the zwitterions in a controlled manner upon covering the hydrogel with water (Figure 5d). Depending on the compound used as payload, 30-70 % of the zwitterion release into water in less than 24 h.

Alternatively, stimulated release is observed in the presence of saline solutions with a concomitant reduction in the total amount discharged. Thus, while 47 % of L-carnitine is released in water within 10 hours, in a NaCl 0.3 M media, the same amount is reached in 2 hours although in this case part of the payload remain entrapped in the shrunken hydrogel. In all cases tested, the release follows a pseudo second-order kinetic model, characteristic of solid-liquid sorption processes (Figure S15).

The above experiments highlight the structural, thermal and mechanical differences existing between hydrogels **1A**, **1B** and **2A**. These differences arise from the different contributions of the aryl squaramide substituents. The results obtained provide clear evidence that parallel stacking of the 4-nitrophenyl squaramide governs the aggregation of **1** to **1A**. However, the two CF₃ substituents of the 3,5-bistrifluoromethylphenyl squaramide can establish additional C_A-H...F-C(sp³) and C(sp³)-F...F-C(sp³) interactions. In addition to aromatic stacking, fluorine interactions likely contribute to the aggregation of **2**, as has been observed in the solid-state structure of a related squaramide derivative.^[13b]

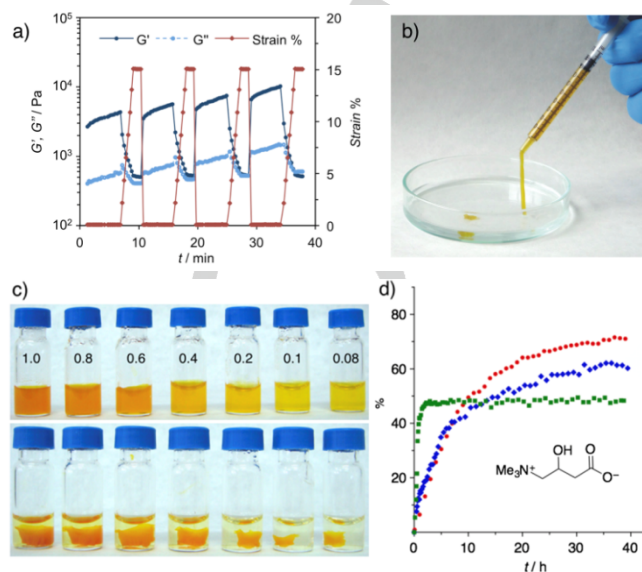


Figure 5. (a) Rheology time sweep of **1A** (2 % w/v) at 1 Hz applying four cycles of low strain (0.1 %, 6 min) and high strain (15 %, 90 seconds) at 25 °C. (b) Photograph of a hydrogel **1A** (1.0 % w/v) (1 Hz; $G' \approx 400$ Pa, $G'' \approx 57$ Pa) indicating fluid-like properties. (c) Photograph of hydrogels **1A** (500 μ L) before and after the addition of a NaCl solution (50 μ L, 50 mM) showing shrinking at equilibrium (24 h). The concentration of **1A** (% w/v) is labeled on the vials. (d) Comparative release profile of L-carnitine (69 mM) loaded in **1A** (0.6 % w/v, 100 μ L) at 25 °C and covered by 500 μ L of water (red), 100 mM NaCl (blue) and 300 mM NaCl (green), respectively.

Conclusions

In conclusion, we have demonstrated the formation of hydrogels based on squaramide-squaramate ensembles. We have utilized squaramic acids for the first time as the hydrophilic component of minimalist LMWHs, joined to an aryl squaramide unit as the hydrophobic moiety. The aryl substituents (NO₂ and CF₃) induce dramatic thermal and mechanical differences in the aggregation of the hydrogels. The hydrogel containing the 4-nitrophenyl squaramide motif is thermoreversible, thixotropic, injectable and can be loaded with a substantial amount of zwitterionic biomolecules, rarely used as payloads. Overall, we have demonstrated the technological potential of the squaramide-squaramate couple as a new tool for the design of supramolecular hydrogels.

Acknowledgements

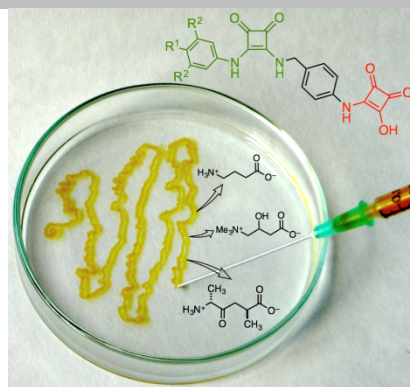
We thank the Ministry of Economy and Competiveness for financial support (grant ref. CTQ2014-57393-C2-1-P) and C. L. thanks Government of the Balearic Islands (CAIB) and European Social Funds (FSE) for a predoctoral fellowship. We thank Dr. G. Martorell and Dr. R. Gomila (SCT-UIB) for assistance with HRMS measurements, and Prof. Priam Villalonga and Dr. Guillem Ramis for evaluation of cytotoxicity.

Keywords: hydrogel • squaramide • squaramic • stacking • supramolecular aggregation

- [1] a) M. J. Webber, E. A. Appel, E. W. Meijer, R. Langer, *Nat. Mater.* **2016**, *15*, 13-26; b) R. Dong, Y. Pang, Y. Su, X. Zhu, *Biomater. Sci.* **2015**, *3*, 937-954; c) D. Yuan, B. Xu, *J. Mater. Chem. B.* **2016**, *4*, 5638-5649; d) M. D. Segarra-Maset, V. J. Nebot, J. F. Miravet, B. Escuder, *Chem. Soc. Rev.* **2013**, *42*, 7086-7098; e) X. Du, J. Zhou, J. Shi, B. Xu, *Chem. Rev.* **2015**, *115*, 13165-13307.
- [2] For recent examples, see: a) E. V. Alakpa, V. Jayawarna, A. Lampel, K. V. Burgess, C. C. West, S. C. Bakker, S. Roy, N. Javid, S. Fleming, D. A. Lamprou, *Chem.* **2016**, *1*, 298-319; b) M. J. Webber, E. A. Appel, E. W. Meijer, R. Langer, *Nat. Mater.* **2016**, *15*, 13-26, and references therein; c) H. Shigemitsu, T. Fujisaku, S. Onogi, T. Yoshii, M. Ikeda, I. Hamachi, *Nat. Protoc.* **2016**, *11*, 1744-1756.
- [3] N. Singh, K. Zhang, C. A. Angulo-Pachón, E. Mendes, J. H. van Esch, B. Escuder, *Chem. Sci.* **2016**, *7*, 5568-5572.
- [4] M. D. Konieczynska, J. C. Villa-Camacho, C. Ghobril, M. Perez-Viloria, K. M. Tevis, W. A. Blessing, A. Nazarian, E. K. Rodriguez, M. W. Grinstaff, *Angew. Chem. Int. Ed.* **2016**, *55*, 9984-9987.
- [5] a) L. A. Estroff, A. D. Hamilton, *Chem. Rev.* **2004**, *104*, 1201-1218; b) S. S. Babu, V. K. Praveen, A. Ajayaghosh, *Chem. Rev.* **2014**, *114*, 1973-2129.
- [6] a) Y. Li, F. Wang, H. Cui, *Bioeng. Transl. Med.* **2016**, *1*, 306-312; b) J. W. Steed, *Chem. Soc. Rev.* **2010**, *39*, 3686-3699; c) Y. Wan, Z. Wang, J. Sun, Z. Li, *Langmuir.* **2016**, *32*, 7512-7518; d) R. Liang, Z. Luo, G. Pu, W. Wu, S. Shi, J. Yu, Z. Zhang, H. Chen, X. Li, *RSC Adv.* **2016**, *6*, 76093-76098.
- [7] V. Saez Talens, P. Englebienne, T. T. Trinh, W. E. Noteborn, I. K. Voets, R. E. Kieltka, *Angew. Chem. Int. Ed.* **2015**, *54*, 10502-10506.]
- [8] a) A. Portell, M. Font-Bardia, R. Prohens, *Cryst. Growth Des.* **2013**, *13*, 4200-4203; b) R. Prohens, A. Portell, M. Font-Bardia, A. Bauzá, A. Frontera, *Cryst. Growth. Des.* **2014**, *14*, 2578-2587, c) C. Estarellas, M. C. Rotger, M. Capó, D. Quiñero, A. Frontera, A. Costa, P. M. Deyà, *Org. Lett.* **2009**, *11*, 1987-1990; d) C. Rotger, B. Soberats, D. Quiñero, A. Frontera, P. Ballester, J. Benet-Buchholz, P. M. Deyà, A. Costa, *Eur. J. Org. Chem.* **2008**, 1864-1868.
- [9] a) B. Soberats, L. Martínez, E. Sanna, A. Sampedro, C. Rotger, A. Costa, *Chem. Eur. J.* **2012**, *18*, 7533-7542; b) J. Schiller, J. V. Alegre-Requena, E. Marqués-López, R. P. Herrera, J. Casanovas, C. Alemán, D. Díaz Díaz, *Soft. Matter.* **2016**, *12*, 4361-4374.
- [10] Squaramic acid stands for 3-hydroxy-4-amino-cyclobut-3-ene-1,2-dione. a) C. López, M. Vega, E. Sanna, C. Rotger, A. Costa, *RSC Advances.* **2013**, *3*, 7249-7253; b) J. Xie, A. B. Comeau, C. T. Seto, *Org. Lett.* **2004**, *6*, 83-86.
- [11] E. Sanna, L. Martínez, C. Rotger, S. Blasco, J. González, E. García-España, A. Costa, *Org. Lett.* **2010**, *12*, 3840-3843.
- [12] M. Ximenis, E. Bustelo, A. G. Algarra, M. Vega, C. Rotger, M. G. Basallote, A. Costa, *J. Org. Chem.* **2017**, *82*, 2160-2170.
- [13] a) V. Amendola, G. Bergamaschi, M. Boiocchi, L. Fabbri, M. Milani, *Chem. -Eur. J.* **2010**, *16*, 4368-4380; b) R. B. Elmes, P. Turner, K. A. Jolliffe, *Org. Lett.* **2013**, *15*, 5638-5641.
- [14] C. López, E. Sanna, L. Carreras, M. Vega, C. Rotger, A. Costa, *Chem. -Asian. J.* **2013**, *8*, 84-87.
- [15] X. Ni, X. Li, Z. Wang, J. P. Cheng, *Org. Lett.* **2014**, *16*, 1786-1789.
- [16] Z. Chen, A. Lohr, C. R. Saha-Möller, F. Würthner, *Chem. Soc. Rev.* **2009**, *38*, 564-584.
- [17] H. Ye, C. Owh, X. J. Loh, *RSC Adv.* **2015**, *5*, 48720-48728.

COMMUNICATION

Smart supramolecular hydrogels, based on squaramides and squaramate synthons were developed. A hydrogel ($R_1 = \text{NO}_2$, $R_2 = \text{H}$) is thermoreversible, thixotropic and injectable. It can be loaded with zwitterions and displays ion-stimulated shrinking and release of the payload. This combination of properties is unusual in supramolecular hydrogels derived from LMWH.



Carlos López, Marta Ximenis,
Francisca Orvay, Carmen Rotger and
Antonio Costa*

Page No. – Page No.

**Supramolecular Hydrogels Based on
Minimalist Amphiphilic Squaramide-
Squaramates for Controlled Release
of Zwitterionic Biomolecules**